Welding Aluminum Sheet Using a High Power Diode Laser

A look at fillet welds in lap joints of aluminum Alloy 5182

BY K. HOWARD, S. LAWSON, AND Y. ZHOU

ABSTRACT. The feasibility has been studied of producing lap-fillet welds in lap joints in Alloy 5182 aluminum sheet with a high-power diode laser. Laser energy absorption and bead formation were found to be very sensitive to surface conditions. Sanding and cleaning of workpieces reduced the weld area significantly compared to as-received sheet surface conditions. Cleaning, however, reduced oxide tail defects and consistently produced welds with increased throat. The addition of dark substances to the surface of the sheets was shown to increase absorptivity, although not necessarily increasing the weld throat. Effects of laser beam presentation were studied, and operating ranges were defined. Mechanisms of pool development in fillet welds in lap joints were explored. It was found that production of fillet welds in lap joints in aluminum sheet with the diode laser is feasible for industrial use and may be especially useful for welding of hem joints in automotive closure panels.

Introduction

The recent emergence of high-power direct diode lasers into the marketplace has opened interesting and attractive possibilities to sheet metal welding technology. The need to embrace new joining technologies is becoming particularly apparent in the automotive industry, where lightweight materials such as aluminum are becoming more commonly used. The high-power diode laser (HPDL) offers opportunities to meet some of the unique challenges of joining aluminum.

The HPDL offers several advantages over CO_2 and Nd:YAG lasers, which are perhaps the most used in laser welding applications. The wavelength of the HPDL, at 800 nm, corresponds to a higher absorptivity in aluminum than the longer wavelengths of Nd:YAG and CO_2 lasers (Ref. 1). Other attractive features of the HPDL include a much smaller system footprint and increased system efficiency compared to Nd:YAG and CO_2 lasers (Ref. 2). The power density of the diode laser beam limits it to conduction-mode welding applications, which results in a very stable, quiescent weld pool. The absence of violent fluid motion, which is present in keyhole-mode welding (Refs. 3–5), results in a very smooth and attractive weld surface appearance. In addition, the stable conduction mode allows for good control of penetration depth. The small size of the laser head allows for access into many tight areas, and therefore eliminates the need for fiber-optic delivery that is commonly used with Nd:YAG lasers; the ability to weld directly reduces losses of power and therefore supports the high system efficiency of the HPDL.

Butt joint welds with consistent fusion have been produced easily and reliably with the HPDL at the University of Waterloo, as well as by other laboratories (Refs. 6–8). The ease of production of butt joint welds makes the HPDL an excellent candidate for production of tailor welded blanks. Our preliminary results show that overlap welding, however, is not particularly suitable for the HPDL, since the conduction mode-nature of the process makes it difficult to break the stubborn aluminum oxide layer between sheets (Ref. 9).

The HPDL appears to be particularly well suited to fillet welds in lap joints; however, there are many complexities to explore concerning the process and setup. Diode laser welding, therefore, may be very appropriate for production of fillet welds in lap joints in hem joints (Fig. 1) of automotive closure panels, where controlled weld penetration and shape as well as excellent surface appearance are imperative. Research on diode laser welding of aluminum alloys at the University of Waterloo has focussed on fillet welds in lap joints.

Other researchers (Refs. 6–8) have introduced the advantages of the high-power diode laser and its ability to produce welded joints in sheet metal. However, knowledge of the mechanisms of this new process is, so far, very limited. Due to the inherent characteristics of the HPDL, details of the weld pool dynamics and material-surface interactions may be quite different from those occurring in CO_2 and Nd:YAG laser welding processes.

The objective of this research is to consider the feasibility of incorporation of the HPDL welding process into industry, as well as to develop an understanding of the mechanisms of the diode laser welding process and some unique considerations in the use of the process.

KEYWORDS

Fillet Welds in Lap Joints
Aluminum
Weld Throat
Weld Pool
High-Power Diode Laser (HPDL)
Weld Bead Formation

Equipment and Experiment Setup

All welding was performed autogenously using a Nuvonyx ISL-4000L diode laser system mounted on a Panasonic VR-16 welding robot. The Nuvonyx ISL-4000L is a 4-kW AlGaAs diode laser with a wavelength of 800 nm. A rectangular beam of 0.5 x 12 mm at the focal plane is generated by focusing light from four diode arrays of 20 diode bars each. The rectangular beam shape gives the Nuvonyx ISL-4000L the unique ability to perform welding with motion parallel to the long axis of the beam, and operations such as heat treating, cladding, and paint stripping with motion parallel to the short axis of the beam.

Tight, uniform clamping in these experiments was delivered by a fixture as illustrated in the system schematic — Fig. 2. Clamping bars machined from high-strength steel allowed the transfer of strong clamping forces through a thin, streamlined geometry. The design of the

K. HOWARD, S. LAWSON, and Y. ZHOU are with the University of Waterloo, Waterloo, Ont., Canada.

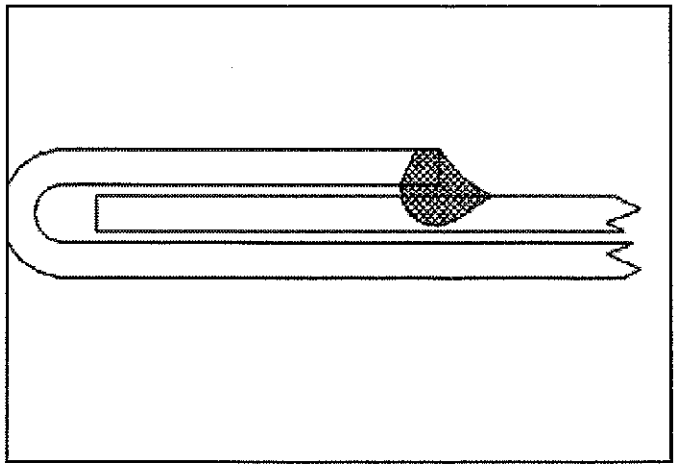

Fig. 1 — Cross section of in lap joints weld configuration.

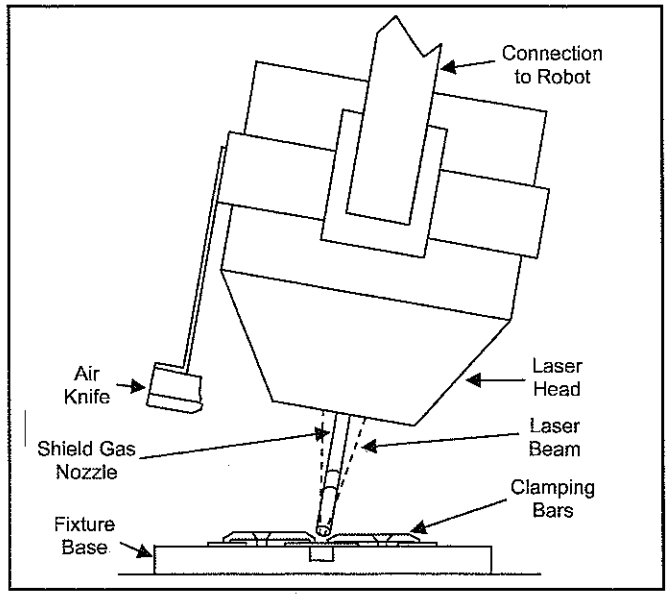

Fig. 2 — Diode laser welding fixture and shielding gas setup.

Table 1 — Density and Composition of Main Alloying Elements for Aluminum Alloys 5182, 6111, and 6013

		Main Alloying Elements (wt-%)			
Alloy	Density ($kg\ m^{-3}$)	Mg	Si	Mn	Cu
5182	2650	4–5	0.2 max	0.2–0.5	Max 0.15
6111	2710	0.5–1	0.6–1.1	0.1–1.1	0.5–0.9
6013	2710	0.8–1.2	0.6–1	0.2–0.8	0.6–1.1

fixture and the clamping bars allowed for full access of the HPDL to the weld joint without interfering with the shielding gas flow or air knife. A 304 stainless steel backing bar was used for all fillet welds in lap joints discussed here, in order to avoid excessive conduction of heat into the backing bar while providing firm clamping support.

Shielding was provided by feeding 99.999% pure argon through a specially designed nozzle. The shield gas nozzle was attached to the bracket surrounding the laser head and angled to provide a laminar flow of gas from the front of the weld pool.

All welding was performed with the laser beam axis tilted laterally at 5 deg or more from the normal to the sheet surface, as shown in Fig. 2, as a precaution to prevent energy from being reflected back into the laser cavity and possibly causing damage.

The majority of fillet welds in lap joints in this study were produced on 1.5-mm-(0.059-in.-) thick 5182-O aluminum alloy. Additional welds were made joining 1.5-mm-thick aluminum Alloy 5182 to 1.5-mm-thick aluminum Alloy 6013 or 1-mm-(0.039-in.-) thick aluminum Alloy 6111. Table 1 lists the chemical compositions and densities of the alloys used in this study (Refs. 10, 11). A constant travel speed of 1 m/min (39.4 in./min) was maintained throughout all of the welding experiments. While much higher welding speeds are possible for joining of thinner sheet material and for butt joint welding, this speed was selected to allow for good consistency of results while varying other welding parameters.

In these experiments, clamping, surface condition, and beam presentation were varied in a systematic manner. The effects of each of these variables were studied mainly by examining the cross sections of welds produced with each set of parameters. Weld cross-sectional area was used as an indicator of absorptivity. Beside weld area and shape, the weld throat measurement was used as an important performance criteria for comparing welding procedures. Weld throat is a direct predictor of weld strength and has been used as a quality indicator for hem welds in industry (Ref. 12).

In a fillet weld of leg length equal to the sheet thickness h, the theoretical throat equals 0.707 h. It has been experimentally verified (Ref. 13) that when material properties of weld metal and base metal are similar, transverse fillet welds with actual throats smaller than this will generally fail in shear through the weld throat, while larger actual throat will tend to shift the location of overload failure to the base metal. Therefore, in this work, the acceptance criterion for welding procedures (sets of specific welding parameters) included the ability to consistently generate a minimum weld throat of 0.707 h. Weld throat was measured using image analysis software as the shortest distance between the edge of the sheet interface (or any existing oxide tail) and the weld bead surface.

Challenges in Diode Laser Welding of Aluminum

A main challenge in applying most joining technologies to aluminum is its tendency to form a thick, coherent oxide layer. This oxide layer has a melting temperature much higher than that of aluminum itself, and it has significant mechanical strength. The oxide layer can therefore remain as a solid film, even when metal surrounding it is molten, resulting in severe incomplete fusion defects. In addition, a thick oxide layer can act as an insulator to heat flow, which is a significant issue in a conduction mode welding process. Figure 3 shows an example of a weld with lack of heat transfer from top sheet to bottom sheet and severe oxide tail defects.

It has been found that employing aggressive clamping along the length of the joint can reduce the problems with oxide tails and heat conduction (Refs. 9, 14).

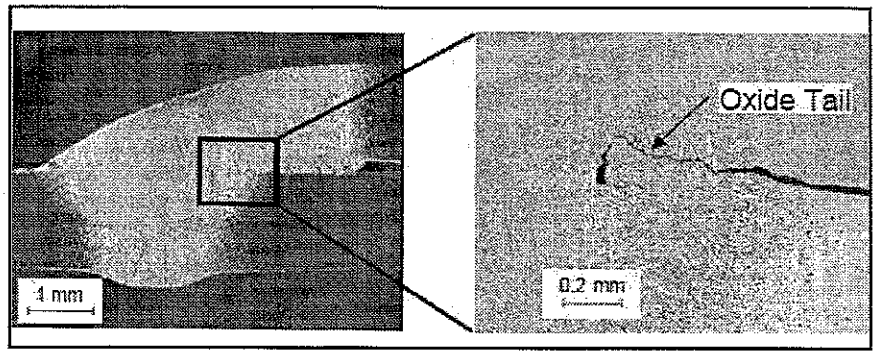

Fig. 3 — Fillet weld in lap-joint with insufficient clamping showing oxide tail defect. Travel speed 1 m/min.

The issues associated with oxide layers are not as significant with keyhole mode laser welding processes, since the drilling action of the vaporized keyhole in the material will tend to break up and disperse oxide layers allowing good fusion. The same calm nature of the conduction weld pool that allows for a smooth, attractive surface appearance and controlled weld shape also reduces the ability of the weld pool to disrupt an oxide barrier.

The absorptivity of aluminum at 800 nm is quoted at 13% for a pure, polished aluminum surface in a vacuum with no oxide layer present (Ref. 1). In practice, the actual absorptivity will be influenced by the presence of an oxide layer, other surface contaminants, and surface roughness (Ref. 3).

The effects of surface condition on laser welding processes have been investigated by various researchers (Refs. 3, 15, 16). Some have stated (Ref. 16) that surface conditions have little effect on laser welding and cutting operations since the surface of the workpiece melts or is vaporized soon after beam irradiation starts. Yet others (Refs. 3, 15) have stated that increasing surface roughness by sanding, for example, will increase the absorptivity of the material. Surface conditions can be expected, however, to play a larger role in conduction mode than in keyhole mode welding, since the formation of a keyhole increases the energy absorbed by multiple reflections and plasma interactions inside of the keyhole (Refs. 3, 4). The complexities of the laser beam/surface interaction with diode laser welding have yet to be studied in detail.

Results

Effect of Surface Condition

Effect of Cleaning

Six different surface preparation conditions were considered in order to gain an understanding of surface effects on weld properties. Samples were prepared either with the as-received surface condition and as-sheared edge, with the burred face of the upper sheet sanded, or with all sides involved in the joint of both sheets sanded, as shown in Fig. 4. The three sanding conditions shown were then repeated, followed by wiping all surfaces with acetone. In this investigation, "sanding" denotes dry manual grinding with a 240-grit silicon carbide metallographic abrasive paper until no traces of original surface color or texture remained. Surface examination after sanding confirmed that no significant quantities of debris or abrasive were embedded. All welds were performed at 4 kW power and speed of 1 m/min.

It can be seen in Figs. 5 and 6 that as the amount of cleaning increased, the weld area decreased. This implied that the surface conditions had a large effect on the overall absorptivity of the system. In addition, as expected, the oxide tail length decreased as amount of cleaning increased. The combined trends of decreasing weld area and decreasing oxide tail led to a slight overall increase in weld throat as cleaning was increased. Although increased cleaning appeared to decrease the thermal efficiency of the welding process, the benefit of reduction in oxide tail outweighed the disadvantage of decreased absorptivity.

It was clear that in the case of diode laser welding on aluminum, the surface condition did have a significant effect on the absorptivity of the material and that sanding and cleaning the surface did not increase the absorptivity of the aluminum sheet surface, but rather decreased it. This suggested that an oxide layer and/or other surface contaminants present on the as-received sheet surface were acting to increase the absorptivity. When the surface was sanded, the surface oxide was disrupted, and it was expected that it was removed to a large extent.

Although new oxide always forms instantaneously on aluminum in air, the newly formed oxide layer was expected to be much thinner. Although the surface roughness was increased by sanding, the

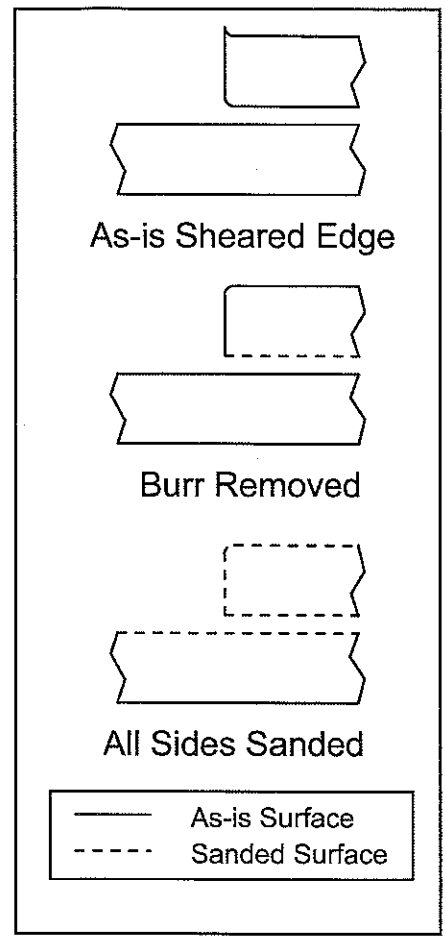

Fig. 4 — Sanding and cleaning conditions.

absorptivity decreased as a result of reducing the oxide layer and surface contaminants. It appeared that for the diode laser welding process on aluminum, the effect of reducing the surface contaminants was much more significant than the effect of increasing surface roughness.

As mentioned previously, Xie and Kar (Ref. 16) have suggested that surface conditions of the solid material do not largely affect the laser welding process, since most of the beam interaction is with the molten pool. However, a later work by the same authors (Ref. 17) found that the presence of surface oxidation had a measurable influence on the absorption of laser energy by steel sheets. Ono et al. (Ref. 18) and Fujii et al. (Ref. 19) have also found that existing oxide layers on steel and aluminum influenced both energy absorption and fluid flow during welding.

Evidence of a continuous and coherent oxide layer remaining on the surface of the weld pools has been observed in the present study. For example, Fig. 7 shows the surface of a bead-on-plate weld. A shiny track in the center of the weld surface can

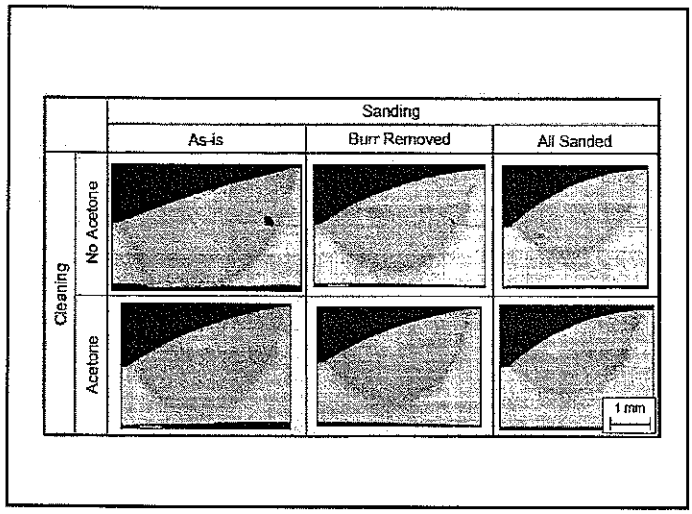

Fig. 5 — Effect of cleaning on weld cross sections. Fillet welds in lap joints on 1.5-mm-thick aluminum Alloy 5182 at 1 m/min.

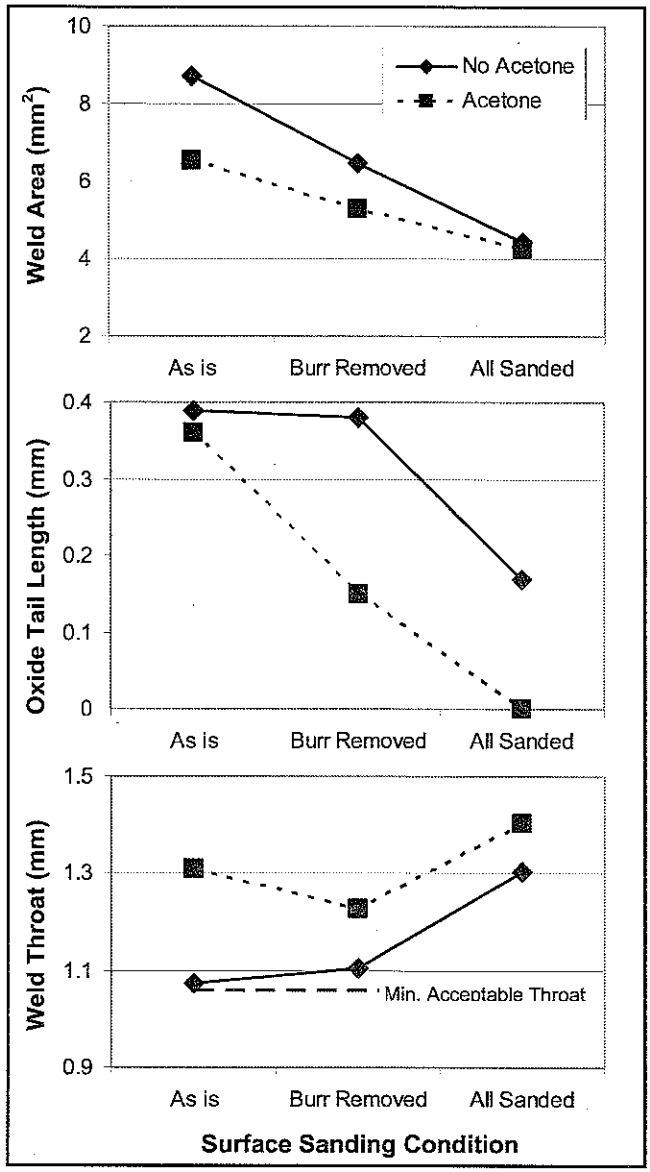

Fig. 6 — Effect of cleaning on weld cross-sectional area, oxide tail length, and weld throat. Fillet welds in lap joints on 1.5-mm-thick aluminum Alloy 5182 at 1 m/min.

be seen where the oxide layer has apparently been disrupted near the laser impingement, possibly due to high temperature at laser impingement, fluid motion, or volumetric expansion of the liquid. However, the remainder of the weld pool has remained covered in a solid oxide layer that has rippled as the weld progressed, but was not broken.

Figure 8 shows the top surface of a fillet weld in a lap joint made with an as-received surface condition. The marks on the surface of the oxide layer showing the rolling direction can clearly be seen on the surface of the weld bead. In addition, some scratches that existed on the surface of the bottom sheet prior to welding have remained intact and terminate at the weld center. The oxide layer of the bottom sheet has been pushed up by the forming weld pool, while the oxide layer on the top sheet has been pulled down, with a shiny track in the center of the weld bead.

Effect of Surface Coatings

The apparent increase in reflectivity with surface cleaning suggested that surface absorptivity could be increased by coating surfaces with substances that are relatively inactive chemically, but dark at visible wavelengths. In Fig. 9, surfaces were sanded and cleaned with acetone (A), and then coated by rubbing with a standard HB clay-graphite pencil (B) or a permanent black felt-tip marker (C). It was seen that the area of the weld with pencil was significantly larger than the weld made on cleaned sheets. Although the weld made with marker on the surface showed porosity caused by decomposition of the surface coating, the weld area was even larger than with pencil.

Measurements (Fig. 10) of these cross sections, however, revealed that although welds produced with coatings had a much larger cross-sectional area, the geometries of the welds were such that the weld throat was not significantly increased compared to welds made with cleaned surfaces. The increased melting did not contribute to increasing the strength of the welds; however, this increased absorptivity may be useful in working to increase welding speed. The coating of sheet surfaces with materials to increase the surface absorptivity is a promising possibility for use of the HPDL in industry.

Effects of Beam Presentation

Effect of Lateral Position and Incident Angle

For any fusion welding process producing fillet welds in lap joints, the positioning of the energy source in relation to the edge of the upper sheet has a major effect on weld bead shape and quality. For this reason, the weld shape and size with respect to beam presentation was examined. In this test series, all coupons for welding had the same surface preparation. For consistency, all sheets were sanded on all sides and cleaned with acetone before welding. Preliminary work had shown that small changes in working distance did not have a large effect on the bead cross section (Ref. 9). Therefore, in order to simplify the experimental matrix, the z position of the focal point was held constant at the center of the top sheet edge. The incident angle of the beam axis and its position in the x direction were varied, as shown in Fig. 11. Cross sections of the welds, as shown in Fig. 12, were examined and the weld throats were measured (Fig. 13).

When a suitable incident angle was used, a tolerance window of approximately 1 mm width was found for acceptable welds in terms of lateral positioning of the beam with respect to the edge of the top sheet. A no-

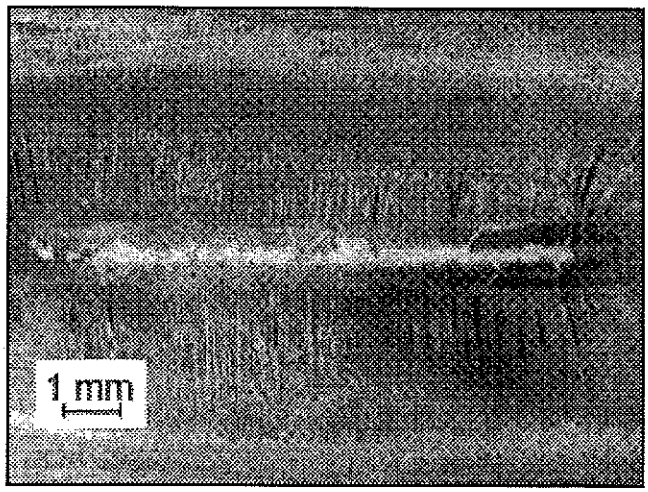

Fig. 7 — Surface of a bead-on-plate weld showing disruption of the oxide layer on the weld center.

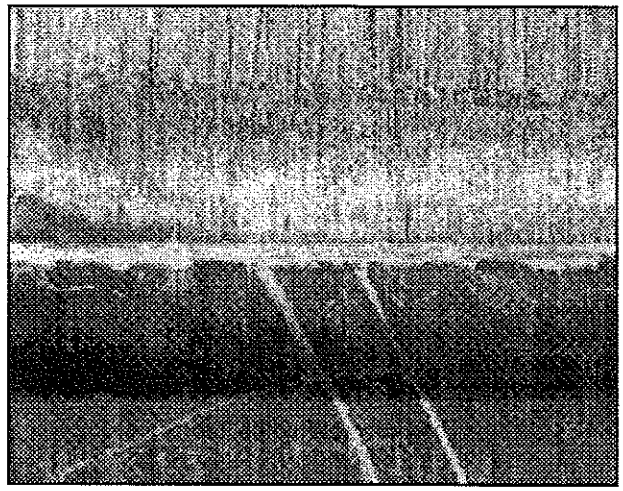

Fig. 8 — Surface of a fillet weld in lap joint with as-received surface condition, showing preservation of the native oxide layer on the bead surface, complete with original surface scratches and rolling texture.

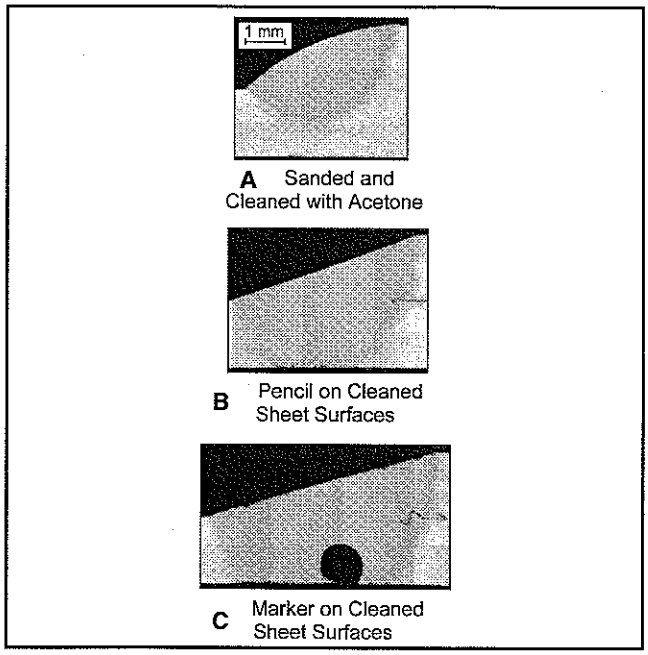

Fig. 9 — Effect of surface coatings on fillet welds in lap joints, 1.5-mm-thick aluminum Alloy 5182 at 1 m/min.

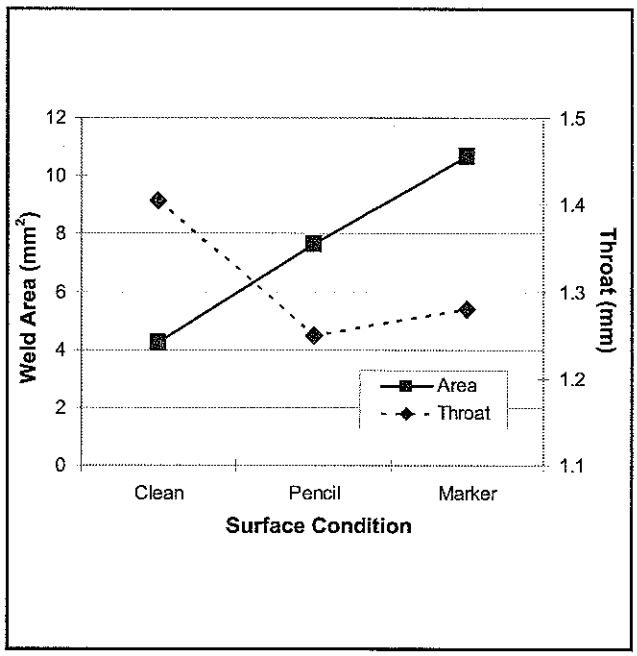

Fig. 10 — Effect of surface coatings on weld cross-sectional area and weld throat, 1.5-mm-thick aluminum Alloy 5182 at 1 m/min.

ticeable trend in shape of the welds could be seen. As the beam moved from impinging mainly on the top sheet toward primarily heating the bottom sheet, the surface of the welds changed from being convex to concave, respectively. Incomplete fusion resulted when the beam was positioned too far in either direction from the edge of the top sheet. There were no strong trends in weld area or oxide tail length with change in beam presentation.

Effect of Beam Twist Angle

The effect of a beam twist angle, as illustrated in Fig. 14, was investigated. Beam twist angles of ±5 deg about the beam's z axis were used, while varying lateral position of the focal point. An incident angle of 20 deg was maintained for all tests, since this produced desirable results in previous experiments. The cross sections of those experiments that produced fused welds are shown in Fig. 15. Introducing twist angle decreased the process tolerance box, enhanced the shape change from convex to concave with change in lateral position, and reduced consistency and repeatability. In fact, of the welds shown in the array of Fig. 15, only the specimen made at –5 deg twist angle with centered lateral position achieved an acceptable throat thickness.

By twisting the rectangular beam of the HPDL, the distribution of the heat source was essentially widened. Eagar and Tsai (Ref. 20) have found that as the distribution of any welding heat source becomes more diffuse, the melting efficiency decreases, reducing the weld size for the same heat input. Alignment of the beam axis to the welded joint is, therefore, very important in HPDL welding.

Discussion

Absorptivity, Joint Geometry, and Weld Throat

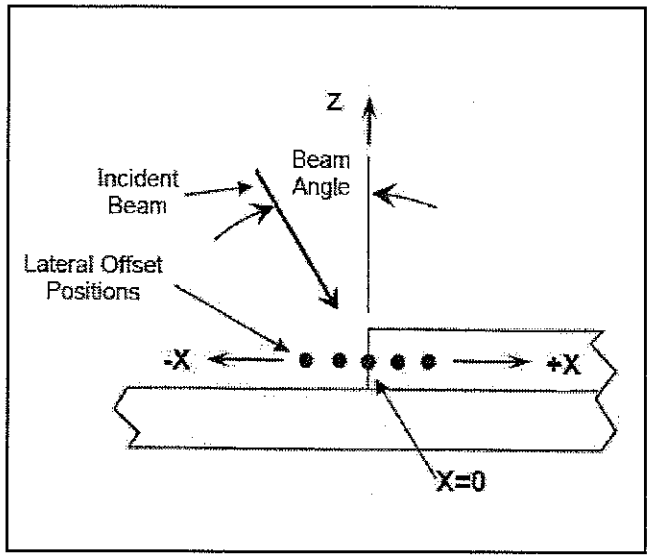

Fig. 11 — Sketch of beam presentation positions for lap-fillet welds with diode laser.

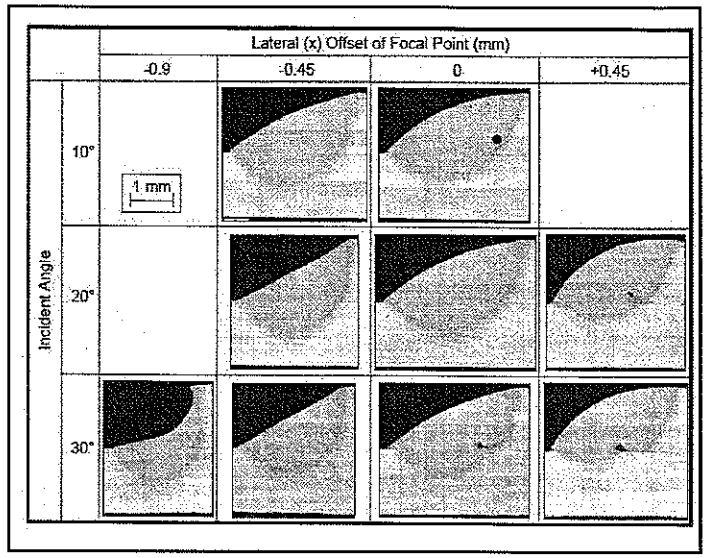

Fig. 12 — Effect of beam presentation on weld cross-sectional area, 1.5-mm-thick aluminum Alloy 5182 at 1 m/min.

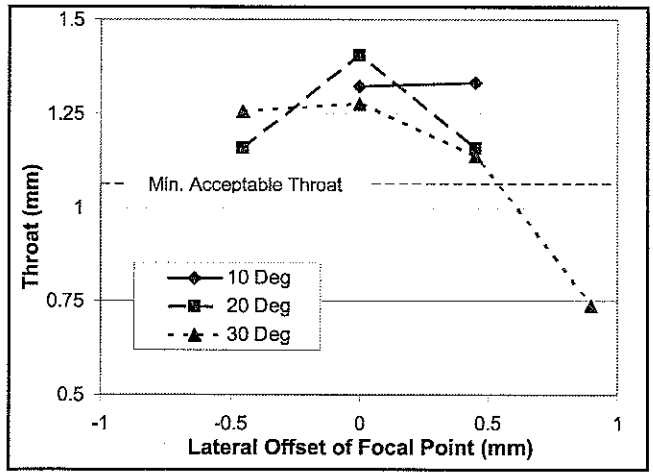

Fig. 13 — Effect of beam presentation on weld throat, 1.5-mm-thick aluminum Alloy 5182 at 1 m/min.

Absorptivity is an important factor in laser welding processes, as greater absorptivity will have a strong influence on the process efficiency and weld cross-sectional area attainable at a given travel speed. Another important consideration, however, is the geometry of the fusion area. Since the weld throat is the smallest area through which a load is transferred through the joint, it is a more important geometrical measurement than weld area.

As absorptivity was increased in the case of fillet welds in lap joints (Fig. 9), the weld area subsequently increased significantly; however, the weld throat did not change considerably. In fact, increase of weld area without a corresponding increase in weld throat was expected to reduce the strength of the joint, since the increase of specific energy input that is implied by greater melted area could contribute to additional local strength loss, the amount dependent on the alloy and temper. Note that detrimental effects of welding on the base metal would be amplified in heat treatable aluminum alloys. Therefore, increasing the absorptivity of the material by the addition of substances to the surface will not necessarily improve joint quality unless the energy can be directed in a manner that results in increased weld throat or can be used to increase welding speed to produce the same weld throat.

Further research on absorptivity and heat flow of diode laser welds in aluminum is underway at the University of Waterloo.

Mechanism of Weld Pool Development

An understanding of the mechanisms of weld bead formation is desirable to aid in the development of process improvements and future industrial procedure development.

In order to gain an understanding of the mechanism of weld bead formation, craters formed at weld termination were successively sectioned at increments of 3 mm from the first sign of melting at the leading edge of the weld pool. Since the leading end of the weld represents the front of the weld pool as it travels along the sheet edge, cross sections through the weld craters should give insight into the stages of weld pool development. Welds were made under different cleaning conditions, while maintaining an incident angle of 20 deg and focal point at the center of the edge of the top sheet.

Figure 16 shows a series of cross sections through the end of a weld with no cleaning, and cross sections of a weld made after sanding all surfaces and cleaning with acetone.

Investigation of the cross sections through weld craters showed that the sequence of weld pool development was quite different with varying cleaning conditions. This investigation has led to the following discussion on the mechanisms of weld pool development.

Cleaning of All Surfaces Prior to Welding

In the weld produced after sanding all surfaces and cleaning with acetone, melting was first seen on the top sheet edge, with no evidence of melting on the bottom sheet at the leading edge of the weld pool. The confinement of melting to the top sheet may have been a result of increased local absorptivity due to roughness remaining on the sheared edge. Once melting of both top and bottom sheets had begun, fusion into a combined weld pool was almost immediate. At 6 mm from the front of the weld pool, good fusion was already seen, with only small traces of oxide layer remaining. The thin oxide layer newly formed within a few minutes of

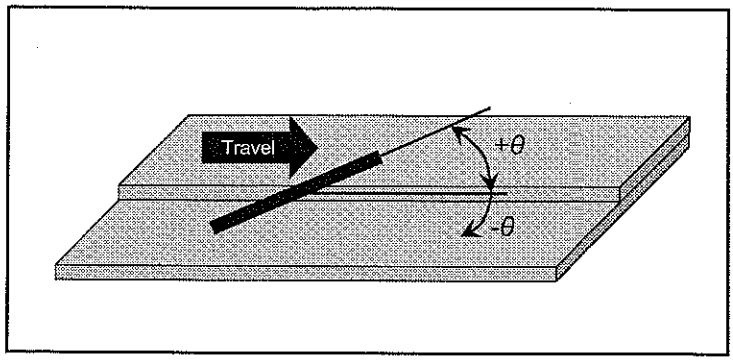

Fig. 14 — Sketch of beam twist angle in welding fillet welds in lap joints with diode laser.

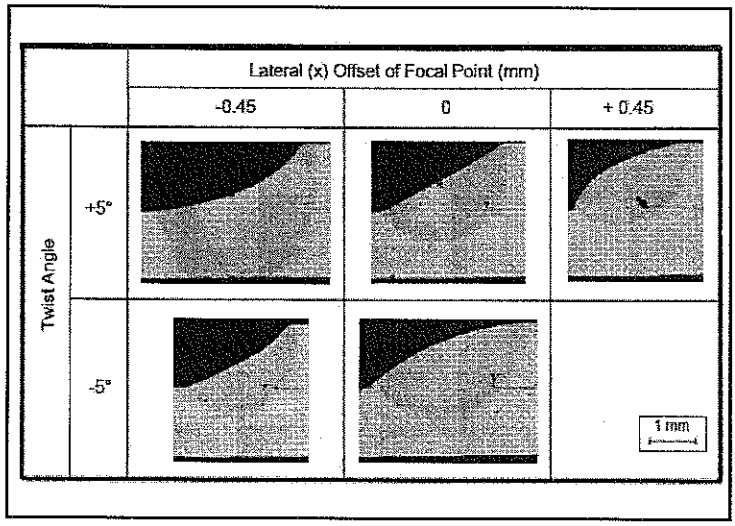

Fig. 15 — Effect of beam twist angle and lateral beam position on weld cross sections, 1.5-mm-thick aluminum Alloy 5182 at 1 m/min.

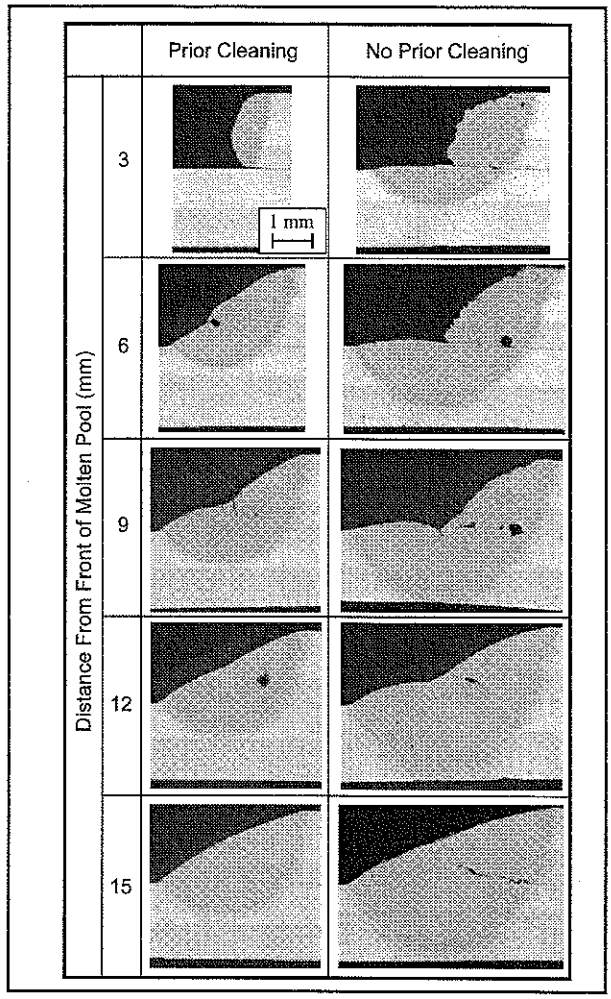

Fig. 16 — Cross sections through fillet weld in lap joints craters showing weld pool development, 1.5-mm-thick aluminum Alloy 5182 at 1 m/min.

sanding the surface appeared to be thin enough and weak enough to be easily broken and washed away by any fluid motion.

The section at 6 mm from the front of the weld bead exhibited pushing of the remaining oxide layer upward, as also seen in the weld without cleaning, thus suggesting that the fluid motion pattern likely behaved in a similar manner for both cleaning conditions. This fluid motion is further discussed in reference to the weld produced without prior cleaning.

After initial fusion, the surface gradually assumed the smooth convex shape; however, the depth and shape of penetration did not change significantly beyond 6 mm from the leading edge of the weld pool.

The proposed mechanism of bead formation with cleaned sheet surfaces is as follows:

1. Melting of the top sheet edge begins early in the beam interaction with little melting of the bottom sheet.

2. Once melting of top and bottom sheets is established, the thin oxide layer is easily broken due to fluid motion and fusion is almost immediately achieved. Any remaining oxide layer is washed away.

3. The weld bead develops into a smooth convex shape.

No Cleaning Prior to Welding

When no cleaning of the aluminum sheets had been performed prior to welding, the sheet surfaces had a relatively thick oxide layer and significant presence of surface contaminants such as dirt and grease. In addition, the edge of the top sheet of the lap fillet weld was in the sheared condition with no further processing. Early in the beam interaction, melting of both the top and bottom sheets was observed; in fact, offset between beginning of melting on the top sheet and beginning of melting of the bottom sheet was about 3 mm in the uncleaned condition compared to 6 mm for welds made after sanding and cleaning with acetone. However, no fusion was seen for the first 6 mm of the weld bead in the uncleaned condition, as the thick oxide layer acted as a barrier to fusion.

At a distance of 9 mm into the weld bead, the oxide layer was broken, and fusion was achieved. Even after fusion, however, the thick oxide layer persistently remained in the weld bead, reducing the weld throat. The fusion observed at 9 mm from the front of the weld bead appeared to be due to gas bubbles formed at the oxide tail attempting to float out of the weld pool and disrupting the oxide tail as a result of the motion.

Prior to fusion, the weld pool of the bottom sheet was seen to be pushed upward. After fusion in this weld, the oxide tail was seen to be pushed upward as well. Thermal expansion of weld metal was

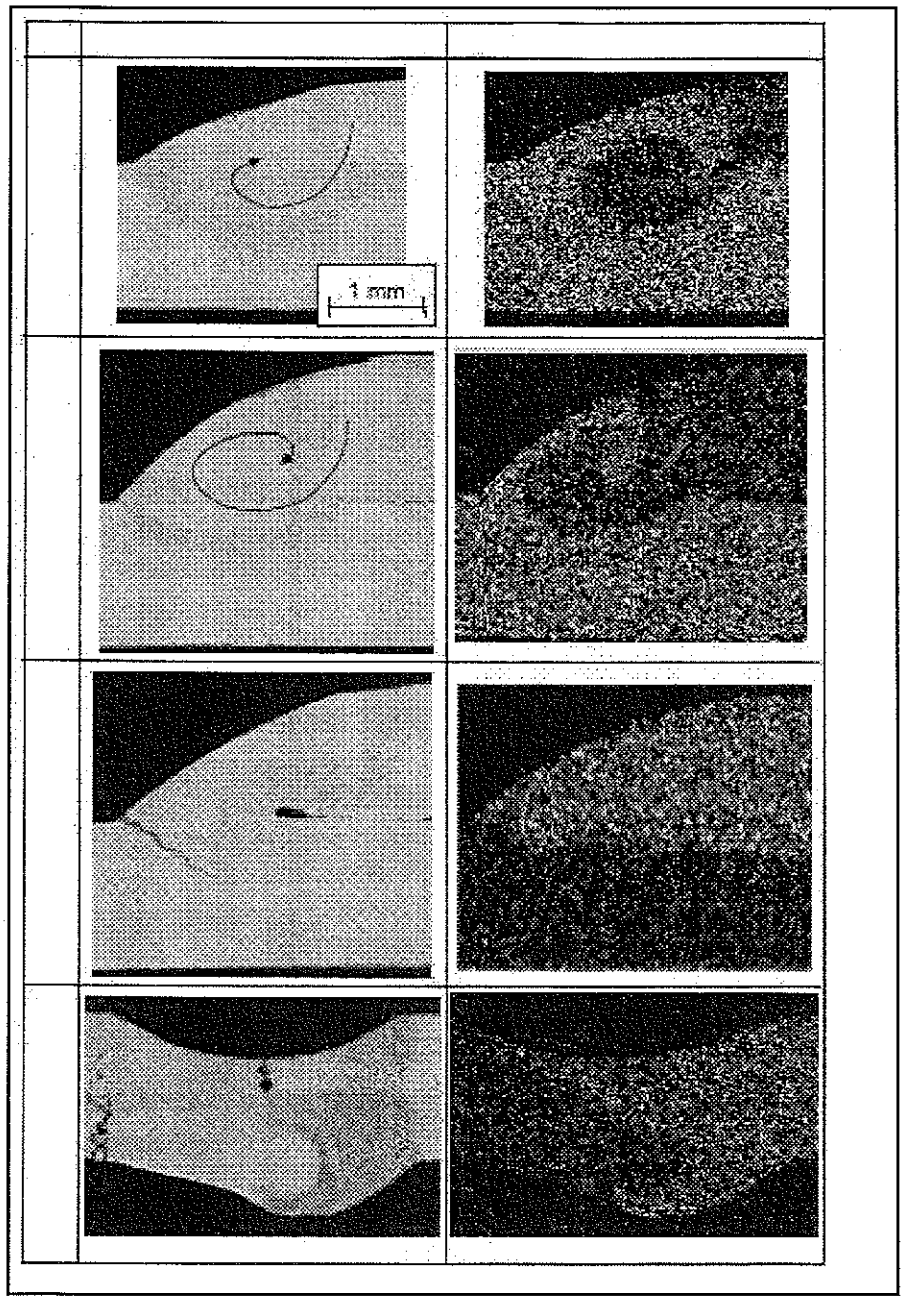

Fig. 17 — Fillet in lap joints and butt joint welds between 5xxx and 6xxx series aluminum alloys showing mixing in weld pools.

likely a factor in the weld bead development. The extent to which other factors and 3-D fluid motion within the weld pool have influenced the bead development have not been quantified, but are recognized as potential factors.

The proposed mechanism for weld bead formation with no cleaning prior to welding is as follows:

1. Melting of the bottom sheet begins shortly after melting of the top sheet. However, the thick oxide layer envelopes the molten metal of both sheet surfaces and acts as a barrier to fusion.

2. Some event must occur in order to disrupt the oxide layer to allow fusion. Often, gas evolves at the faying surfaces of the oxide layers as a result of heating of surface contaminants. Gas bubbles float toward the surface of the weld pool rupturing the oxide layer and allowing mixing of molten metal from the top and bottom sheets.

3. Without some disruption of the oxide layer, some of the oxide is removed near the surface of the weld pool likely due to high temperature near the point of laser impingement, while the majority of the oxide tail remains intact limiting the extent of fusion and the size of the weld throat.

4. The weld bead develops into a smooth convex shape.

Fluid Flow in HPDL Welds of Aluminum

In order to further investigate the fluid motion in diode laser welds, some samples were made joining aluminum Alloy 5182 to aluminum Alloy 6111 or aluminum Alloy 6013. It can be seen in Table 1 that the most significant difference in alloy composition between the 5xxx and 6xxx series alloys is in the magnesium content. It is also significant that the 6xxx series alloys have higher density than the 5xxx series alloys.

Fillet welds in lap joints between 1.5-mm-thick aluminum Alloy 5182 and 1-mm-thick aluminum Alloy 6111 were made, as well as the same type of welds between 1.5-mm-thick aluminum Alloy 5182 and 1.5-mm-thick aluminum Alloy 6013. Fillet welds in lap joints were produced with the aluminum Alloy 5182 as the bottom sheet and 6xxx series alloy at the top sheet, and vice versa. Butt joint welds were produced between the aluminum Alloy 5182 and aluminum Alloy 6013 to further investigate the fluid flow in diode laser welds.

Magnesium concentration in the weld pools was used as an additional indicator of the mixing of the materials during welding by making energy-dispersive x-ray spectroscopic (EDS) concentration maps. Figure 17 shows optical micrographs of cross sections of the mixed alloy welds described above, as well as EDS maps of magnesium content of each cross section. Areas with a higher concentration of white pixels in the EDS maps indicated areas with higher magnesium content. Thus, areas associated with the aluminum Alloy 5182 appear brighter in the EDS maps.
<Insert Fig. 17, Fig 17.JPG>

As may be seen in Fig. 17A, B, when 6xxx series alloys (more dense) were used as a top sheet in a fillet weld in lap joint, a gently swirled mixing pattern was generated. Arrows have been superimposed on the micrographs of Fig. 17A, B, to indicate the direction of the fluid flow. The EDS magnesium maps show distinct areas of high magnesium content in the fusion zone. This indicated that fluid motion in the weld pool was relatively slow and laminar, as material from the upper and lower sheets did not completely mix together.

When 6xxx series alloys were used as the bottom sheet in a fillet weld in a lap joint (Fig. 17C), no mixing at all was seen; since the more dense alloy was on the bot-

tom, gravity did not induce the molten materials to mix. When aluminum Alloy 5182 and aluminum Alloy 6013 were joined in a butt configuration, the material of the aluminum Alloy 6013 sheet was seen to push the aluminum Alloy 5182 out of the way and upward (Fig. 17D). In the case of the butt joint, the denser 6013 alloy was influenced by gravity to flow downward and displace the less-dense 5182 alloy.

Liquation cracks were observed in the base metal of the 6xxx series alloy in the welds in Fig. 17C, D. 6xxx series alloys are highly susceptible to solidification and liquation cracks (Ref. 21), and since there was no filler metal added, the presence of cracks was not unexpected.

From this series of welds, it was clear that the fluid motion in the weld pool was influenced by small density differences in the alloys being joined. When a denser alloy was placed above a less-dense alloy in a weld joint, gravity influenced the more denser alloy to flow downward in the molten weld pool, displacing the less-dense metal and resulting in a gently swirled mixing pattern. When the less-dense alloy was placed above a denser alloy, no mixing at all was seen. This sensitivity to small density differences indicated that forces other than gravitational acting on the weld pool in diode laser welding of aluminum alloys were very small. These results are consistent with fluid flow that is primarily buoyancy driven.

Discussion of Forces on the Weld Pool

The fluid motion in these diode laser welds of aluminum was very different from fluid motion that is often seen in keyhole-mode laser welding or arc welding processes (Refs. 3, 5, 22, 23). The moving keyhole in keyhole-mode laser welding processes forces liquid metal to flow rapidly around the keyhole (Ref. 22). Since the present experiments were based on conduction-mode welding, this rapid fluid motion and mixing did not occur in the diode laser welds.

Other forces that often act on arc weld pools include Lorentz forces, Marangoni forces, and buoyancy forces. Lorentz forces are present in arc welding processes where the current density gradients in the arc and weld pool interact with the magnetic field generated by the current to generate forces acting away from the surface of the weld pool (Ref. 22). Since there is no arc in laser welding processes, there is no Lorentz force.

Marangoni forces are due to surface tension gradients and act along the surface of a weld pool. Depending on the material properties and surface tension gradients, Marangoni forces can influence fluid to flow in various patterns in the weld pool (Ref. 22). No evidence of fluid flow due to Marangoni forces was observed in the diode laser welds of the present study, and this is not surprising since most of the "free" surface area of these welds was actually covered by an immobile, solid oxide film.

Buoyancy forces are due to density changes of the molten metal. In weld pools of uniform composition, liquid at higher temperatures becomes less dense and thus tends to flow upward, while cooler and therefore denser liquid flows downward. In these experiments, the density differences due to the different alloy compositions overcame buoyancy due to heating, and thus had a stronger influence on fluid motion. In other conduction-mode welding processes where Lorentz forces and Marangoni forces are present, gravity or buoyancy forces tend to be comparatively weak (Ref. 23). Lorentz forces are not expected to be present in diode laser welds, and the sensitivity of fluid motion to density indicated that Marangoni forces were also very weak in diode laser welds on aluminum alloys. Therefore, it was concluded that gravity was the most significant force acting on diode laser welds of aluminum.

Berkmanns et al. (Ref. 24) have found that in diode laser welding of steel, Marangoni forces are the dominant force on the melt pool, and combined with the effects of buoyancy, affect the direction of fluid flow in the weld pool. Fujii et al. (Ref. 19) studied the effects of gravity on fluid motion of weld pools and found that surface tension and buoyancy had the greatest effects on fluid motion in electron beam welds. However, when a solid oxide layer was present on the surface of the weld pool, such as in welding of aluminum, the Marangoni forces were greatly reduced.

Since there are no Lorentz forces in diode laser welding and Marangoni forces are expected to be very small if not nonexistent due to solid aluminum oxide layers on the weld surface, buoyancy forces were expected to be the dominant force in fluid motion in these welds. It has been found that these buoyancy forces are relatively weak and can easily be disrupted by composition differences between workpiece materials.

Summary

Work up to this point indicates that it is feasible to produce good-quality fillet welds in lap joints with the HPDL. Aggressive clamping and controlled cleaning conditions will be imperative to the success of such a process in an industrial application.

Investigation of the effect of surface conditions on welding revealed that absorptivity of the aluminum sheet is very sensitive to surface conditions. The weld cross-sectional area, which was measured as an indication of absorptivity, was reduced both by sanding and cleaning with acetone. Cleaning, however, reduced oxide tails in the welds. The effect of reducing oxide tails was more significant than the effect of reducing weld area, and thus cleaning was found to increase weld throat.

It was found that absorptivity could be increased significantly by applying dark substances to the surface. An important observation, however, was that increasing absorptivity would increase weld area, but not necessarily weld throat. Since weld throat is the important geometrical feature relating to strength, it became clear that increasing absorptivity alone did not immediately increase joint strength.

It was found that lap-fillet welds were best produced with an incident angle of 20 deg and focal point at the center of the edge of the top sheet. Welds with acceptable throat were produced with up to 0.5 mm (0.02 in.) of offset from the centerline in the lateral direction, resulting in a tolerance range of about 1 mm (0.04 in.) in the lateral direction. Introducing a twist angle about the beam axis resulted in wider distribution of heat to the workpiece and, therefore, reduced weld size.

The mechanisms of weld bead formation were investigated, and it was found that weld beads form differently under different cleaning conditions. In welds made with good cleaning, oxide layers were easily broken. In welds made without prior cleaning, thick oxide tails remained in the weld pool, reducing amount of fusion. The expulsion of gas bubbles appeared to be an important part of oxide removal in welds with no prior cleaning. The conduction-mode nature of the diode laser welds combined with lack of Lorentz forces and Marangoni forces resulted in quiescent weld pools with very little fluid motion. What little fluid motion did occur was found to be influenced mainly by buoyancy gradients in the molten weld pool. It was also suggested that 3-D fluid motion in the weld pools was present.

Cleaning prior to welding consistently produced welds with acceptable throat and quality, while welding on material with a thick oxide layer and other surface contaminants produced welds with unpredictable and large oxide-related defects. It is clear that controlling surface condition will be imperative to an industrial application of high-power diode laser welding of aluminum.

Acknowledgments

The authors would like to acknowledge the funding and support from Auto21, one of the Networks of Centres of Excellence

supported by the Canadian Government; the Ontario Research and Development Challenge Fund; and Alcan Inc.

References

1. Zediker, M. 1999. Applications and Benefits of Direct Diode Lasers. *http://www.nuvonyx.com/slide%20show/index.htm.*

2. Zediker, M. S., Haake, J. M., and Cook, C. M. 2000. Laser diode material processing system. *Proc. ICALEO 2000, Laser Applications in the Automotive Industry*, Vol. 91, D1–D8. Eds. Hugel, H., Matsunawa, A., Mazumder, J., and DiPetro, F. Orlando, Fla.: Laser Institute of America.

3. Duley, W. W. 1999. *Laser Welding*. Toronto, Wiley Interscience.

4. Ki, H., Mohanty, P. S., and Mazumder, J. 2000. A self-consistent three dimensional laser keyhole welding model. *Proc. ICALEO 2000, Laser Applications in the Automotive Industry*, Vol. 91, D35–D43. Eds. Hugel, H., Matsunawa, A., Mazumder, J., and DiPetro, F. Orlando, Fla.: Laser Institute of America.

5. Zhao, H., White, D. R., and DebRoy, T. 1999. Current issues and problems in laser welding of automotive aluminum alloys. *International Materials Reviews* 44(6): 238–266.

6. Abe, N., Tsukamoto, M., Morikawa, A., Maeda, K., and Namba, K. 2002. Welding of aluminum alloy with high power direct diode laser. *Trans. JWRI* 31(2).

7. Clarke, J. A. 2001. Aluminum tailor-welded blanks. *Proc. ALAW 2001*, 42–80. Ed. Mazumder, J. Ann Arbor, Mich.: University of Michigan College of Engineering.

8. Herfurth, H. J., and Ehlers, B. 2000. Increased performance broadens processing capabilities of high power diode lasers. *Proc. ICALEO 2000, Laser Applications in the Automotive Industry*, Vol. 91, D9–D18. Eds. Hugel, H., Matsunawa, A., Mazumder, J., and DiPetro, F. Orlando, Fla.: Laser Institute of America.

9. Howard, K., Lawson, S., and Zhou, Y. 2003. Unpublished research, University of Waterloo.

10. *Aluminum for Automotive Body Sheet Panels*. 1998. The Aluminum Association, Publication AT3.

11. *Aluminum 6013 Composition Spec.* 2005. *http://www.matweb.com/search/SpecificMaterial.asp?bassnum=MA6013n.*

12. Forrest, M. G. 2003. Laser beam welding of automotive closure panel hems. *Welding Journal* 82(8): 30–35.

13. Gurney, T. R. 1979. *Fatigue of Welded Structures*, 2d ed. Cambridge, U.K.: Cambridge University Press, pp. 129–131.

14. Howard, K., Lawson, S., and Zhou, Y. 2004. Diode laser welding of aluminum. *Proc. AMT 2004*. Government of Canada Catalogue No. NR15-70/2004E-MRC.

15. Xie, J., and Kar, A. 1999. Laser welding of thin sheet steel with surface oxidation. *Welding Journal* 78(10): 343-s to 348-s.

16. Xie, J., Kar, A., Rothenflue, J. A., and Latham, W. P. 1997. Temperature-dependent absorptivity and cutting capability of CO_2, Nd:YAG and chemical oxygen-iodine lasers. *Journal of Laser Applications* 9(2): 77–85.

17. Xie, J., and Kar, A. 1999. Melting and vaporization for large-area film removal with a chemical oxygen-iodine laser. *Journal of Applied Physics* 82(10): 4744–4751.

18. Ono, K., Adachi, K., Miyamoto, I., and Inoue, T. 2002. Influence of oxide film on weld characteristics of mild steel in CO_2 laser welding. *Journal of Laser Applications* 14(2): 73–77.

19. Fujii, H., Sumi, Y., Yamamoto, T., Kamai, M., and Nogi, K. 2001. Effect of gravity and surface tension on convection in molten pool. *Trans JWRI Special Issue HTC-2000*. Vol. 30: 523–528.

20. Eagar, T. W., and Tsai, N. S. 1983. Temperature fields produced by traveling distributed heat sources. *Welding Journal* 62(12): 346-s to 355-s.

21. Dickerson, P. B. 1993. Welding of aluminum alloys. *ASM Handbook*, Vol. 6, Welding, Brazing and Soldering, pp. 722–739. Materials Park, Ohio: ASM International.

22. Heiple, C. R., and Burgardt, P. 1993. Fluid flow phenomena during welding. *ASM Handbook*, Vol. 6, Welding, Brazing and Soldering, pp. 19–24. Materials Park, Ohio: ASM International.

23. Rohklin, S. I., and Guu, A.C. 1993. A study of arc force, pool depression, and weld penetration during gas tungsten arc welding. *Welding Journal* 72(8): 381-s to 390-s.

24. Berkmanns, J., Danzer, W., and Hartl, J. 2002. Influence of process gases in welding with diode lasers. *Proceedings ICALEO 2002*, 1413–1422. Ed. Yao, Y. L. Orlando, Fla.: Laser Institute of America.

Preparation of Manuscripts for Submission to the *Welding Journal* Research Supplement

All authors should address themselves to the following questions when writing papers for submission to the Welding Research Supplement:

- Why was the work done?
- What was done?
- What was found?
- What is the significance of your results?
- What are your most important conclusions?

With those questions in mind, most authors can logically organize their material along the following lines, using suitable headings and subheadings to divide the paper.

1) **Abstract.** A concise summary of the major elements of the presentation, not exceeding 200 words, to help the reader decide if the information is for him or her.

2) **Introduction.** A short statement giving relevant background, purpose, and scope to help orient the reader. Do not duplicate the abstract.

3) **Experimental Procedure, Materials, Equipment.**

4) **Results, Discussion.** The facts or data obtained and their evaluation.

5) **Conclusion.** An evaluation and interpretation of your results. Most often, this is what the readers remember.

6) **Acknowledgment, References and Appendix.**

Keep in mind that proper use of terms, abbreviations, and symbols are important considerations in processing a manuscript for publication. For welding terminology, the *Welding Journal* adheres to AWS A3.0:2001, *Standard Welding Terms and Definitions.*

Papers submitted for consideration in the Welding Research Supplement are required to undergo Peer Review before acceptance for publication. Submit an original and one copy (double-spaced, with 1-in. margins on 8 ½ x 11-in. or A4 paper) of the manuscript. A manuscript submission form should accompany the manuscript.

Tables and figures should be separate from the manuscript copy and only high-quality figures will be published. Figures should be original line art or glossy photos. Special instructions are required if figures are submitted by electronic means. To receive complete instructions and the manuscript submission form, please contact the Peer Review Coordinator, Doreen Kubish, at (305) 443-9353, ext. 275; FAX 305-443-7404; or write to the American Welding Society, 550 NW LeJeune Rd., Miami, FL 33126.